J|A|C|S
ARTICLES
Published on Web 01/31/2002

A Solid-State ^{17}O Nuclear Magnetic Resonance Study of Nucleic Acid Bases

Gang Wu,* Shuan Dong, Ramsey Ida, and Nitin Reen

Contribution from the Department of Chemistry, Queen's University, Kingston, Ontario, Canada K7L 3N6

Received July 3, 2001. Revised Manuscript Received October 5, 2001

Abstract: We report a systematic solid-state ^{17}O NMR study of free nucleic acid bases: thymine (T), uracil (U), cytosine (C), and guanine (G). Site-specifically ^{17}O-enriched samples were synthesized: [2-^{17}O]thymine (**1**), [4-^{17}O]thymine (**2**), [2-^{17}O]uracil (**3**), [4-^{17}O]uracil (**4**), [2-^{17}O]cytosine (**5**), and [6-^{17}O]guanine monohydrate (**6**). Magic-angle-spinning (MAS) and static ^{17}O NMR spectra were acquired at 11.75 T for compounds **1**−**6**, from which information about the ^{17}O chemical shift and electric field gradient tensors was obtained. Extensive quantum chemical calculations were performed at the B3LYP/6-311++G(d,p) level of theory for ^{17}O NMR properties in various molecular models. The calculated ^{17}O NMR tensors are highly sensitive to the description of intermolecular hydrogen-bonding interactions at the target oxygen atom. A reasonably good agreement between experimental solid-state ^{17}O NMR data and B3LYP/6-311++G(d,p) calculations is achievable only in molecular cluster models where a complete hydrogen-bond network is considered. Using this theoretical approach, we also investigated the ^{17}O NMR tensors in two unusual structures: guanine- and uracil-quartets.

1. Introduction

Nuclear magnetic resonance (NMR) spectroscopy of ^{1}H, ^{13}C, and ^{15}N nuclei has become an indispensable technique for studying nucleic acid structures.[1,2] Despite the fact that oxygen is also an abundant element in nucleic acid molecules, only scattered studies can be found in the literature that employ ^{17}O ($I = {}^{5}/_{2}$) NMR to investigate molecules related to nucleic acids.[3−10] The lack of experimental ^{17}O NMR data is a direct consequence of the fact that it is intrinsically difficult to obtain high-resolution NMR spectra for quadrupolar nuclei. For ^{17}O NMR, two major factors contribute to the practical difficulty. First, the natural abundance of ^{17}O is only 0.037%. Second, the large quadrupole interaction associated with many important oxygen-containing functional groups causes efficient relaxation and, consequently, leads to broadening of ^{17}O NMR signals. This quadrupolar broadening is often so severe for biological macromolecules that ^{17}O NMR spectra (even when they are observable) yield very little site-specific information. As a result, solution ^{17}O NMR has been largely restricted to studies of small molecules.[11]

An alternative approach to traditional solution ^{17}O NMR is to obtain ^{17}O NMR spectra for solid samples. Since quadrupole relaxation times are usually much longer for samples in the solid state than those in solutions, the intrinsic spectral resolution of solid-state ^{17}O NMR spectra is not limited by the molecular weight of the system under observation. In the early 1980s, Oldfield and co-workers[12] demonstrated the utility of central-transition ($m = +{}^{1}/_{2} \leftrightarrow -{}^{1}/_{2}$) ^{17}O NMR spectroscopy for solids. Although in some cases useful information can be extracted from central-transition ^{17}O NMR spectra obtained under the magic-angle spinning (MAS) condition, the residual line broadening due to the well-known second-order quadrupole interaction is often too large to allow a sufficient resolution in MAS spectra. Although the second-order quadrupole interaction can be either completely removed by dynamic-angle spinning (DAS)[13] and double rotation (DOR)[14] techniques or significantly reduced at very high magnetic fields, solid-state ^{17}O NMR has rarely been applied to organic compounds.

* To whom correspondence should be addressed. Phone: 613-533-2644. Fax: 613-533-6669. E-mail: gangwu@chem.queensu.ca.

(1) Wüthrich, K. *NMR of Proteins and Nucleic Acids*; Wiley: New York, 1986.
(2) Evans, J. N. S. *Biomolecular NMR Spectroscopy*; Oxford University Press: New York, 1995.
(3) Burgar, M. I.; Dhawan, D.; Fiat, D. *Org. Magn. Reson.* **1982**, *20*, 184.
(4) Chandrasekaran, S.; Wilson, W. D.; Boykin, D. W. *J. Org. Chem.* **1985**, *50*, 829.
(5) Zhuo, J.-C.; Wyler, H.; Péchy, P.; Dahn, H. *Helv. Chim. Acta* **1994**, *77*, 317.
(6) (a) Schwartz, H. M.; MacCoss, M.; Danyluk, S. S. *Tetrahedron Lett.* **1980**, 3837. (b) Schwartz, H. M.; MacCoss, M.; Danyluk, S. S. *J. Am. Chem. Soc.* **1983**, *105*, 5901. (c) Schwartz, H. M.; MacCoss, M.; Danyluk, S. S. *Magn. Reson. Chem.* **1985**, *23*, 885.
(7) Amantea, A.; Henz, M.; Strazewski, P. *Helv. Chim. Acta* **1996**, *79*, 244.
(8) (a) Coderre, J. A.; Mehdi, S.; Demou, P. C.; Weber, R.; Traficante, D. D.; Gerlt, J. A. *J. Am. Chem. Soc.* **1981**, *103*, 1870. (b) Gerlt, J. A.; Demou, P. C.; Mehdi S. *J. Am. Chem. Soc.* **1982**, *104*, 2848. (c) Petersheim, M.; Miner, V. W.; Gerlt, J. A.; Prestegard, J. H. *J. Am. Chem. Soc.* **1983**, *105*, 6357.
(9) Wilde, J. A.; Bolton, P. H.; Mazumder, A.; Manoharan, M.; Gerlt, J. A. *J. Am. Chem. Soc.* **1989**, *111*, 1894.
(10) (a) Tsai, M.-D.; Huang, S. L.; Kozlowski, J. F.; Chang, C. C. *Biochemistry* **1980**, *19*, 3531. (b) Wisner, D. A.; Steginsky, C. A.; Shyy, Y.-J.; Tsai, M.-D. *J. Am. Chem. Soc.* **1985**, *107*, 2814.
(11) Boykin, D. W., Ed. *Oxygen-17 NMR Spectroscopy in Organic Chemistry*; CRC Press: Boca Raton, FL, 1991.
(12) (a) Schramm, S.; Kirkpatrick, R. J.; Oldfield, E. *J. Am. Chem. Soc.* **1983**, *105*, 2483. (b) Schramm, S.; Oldfield, E. *J. Am. Chem. Soc.* **1984**, *106*, 2502.
(13) (a) Llor, A.; Virlet, J. *Chem. Phys. Lett.* **1988**, *152*, 248. (b) Mueller, K. T.; Sun, B. Q.; Chingas, G. C.; Zwanziger, J. W.; Terao, T.; Pines, A. *J. Magn. Reson.* **1990**, *86*, 470.

10.1021/ja011625f CCC: $22.00

Scheme 1

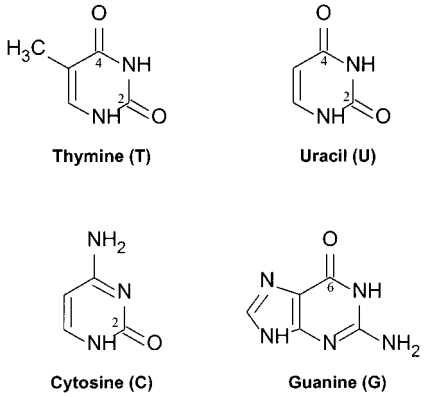

In recent years, there has been a renewed interest in solid-state ^{17}O NMR, primarily because ultrahigh magnetic fields are becoming readily available. In a broader context, this trend is also related to significant advances in NMR methodology for studying half-integer quadrupolar nuclei. The most recent impetus for the rethinking of the solid-state ^{17}O NMR approach comes from the development of the multiple-quantum magic-angle spinning (MQMAS) technique by Frydman and co-workers.[15] This two-dimensional (2-D) NMR method provides a new way of obtaining high-resolution NMR spectra for half-integer quadrupolar nuclei. The utilization of this new approach in ^{17}O NMR was first demonstrated by Wu et al.[16] Recent work from this laboratory has extended this technique to ^{17}O-enriched organic solids.[17]

As a first step to establish solid-state ^{17}O NMR as an effective probe to biomolecular structures, we have recently undertaken a comprehensive NMR study for a variety of ^{17}O-labeled organic compounds.[18−23] For molecules important in the area of nucleic acid chemistry, we also reported preliminary solid-state ^{17}O NMR results for site-specifically ^{17}O-enriched thymine molecules[24] as well as a 2-D ^{17}O MQMAS spectrum for [2,4-$^{17}O_2$]-uracil.[17] Here we report a complete account of solid-state ^{17}O NMR and theoretical investigations on oxygen-containing nucleic acid bases: thymine (T), uracil (U), cytosine (C), and guanine (G) (Scheme 1). More specifically, we synthesized the following ^{17}O-labeled nucleic acid bases: [2-^{17}O]thymine (**1**), [4-^{17}O]thymine (**2**), [2-^{17}O]uracil (**3**), [4-^{17}O]uracil (**4**), [2-^{17}O]-cytosine (**5**), and [6-^{17}O]guanine·H_2O (**6**). By introducing ^{17}O labels into nucleobases in a site-specific fashion, we were able to determine the ^{17}O electric field gradient (EFG) tensor and the chemical shift tensor for all oxygen-containing functional groups in nucleobases. The primary goal of the present study is to produce the first set of fundamental ^{17}O NMR tensors for nucleic acid-related molecules. This set of data provides a foundation for further solid-state ^{17}O NMR studies of larger and more complex nucleic acid systems. Another important feature of the present study is that extensive quantum chemical calculations were carried out to evaluate the effect of intermolecular hydrogen-bonding interactions on ^{17}O NMR properties. Using this theoretical approach, we also evaluated the ^{17}O NMR tensors in two unusual structures: G- and U-quartets.

2. Experimental and Computational Aspects

Synthetic Methods. Water (40.9 atom-% ^{17}O, 1.0 atom-% ^{18}O, lot no. IM1378-14) was purchased from ISOTEC (Miamisburg, Ohio). 2-Thiocytosine, uracil, 4-methyl-thiouracil, thymine, and guanine monohydrate were purchased from Aldrich Chemical Co. and were used without further purification. Routine solution ^1H and ^{13}C NMR experiments were carried out on Bruker Avance-300 and 400 NMR spectrometers. The general procedures used for introducing ^{17}O labels to various positions of the base molecules were similar to those reported previously.[3,25,26] After each reaction, the excessive $H_2{}^{17}O$ was recovered on a high vacuum line. Experimental details for sample synthesis are given below.

[2-^{17}O]Thymine. In a mixture of 1.8 mL of anhydrous dioxane and 30 mg (1.67 mmol) of $H_2{}^{17}O$ was dissolved 180 mg (1.27 mmol) of 5-methyl-2-thiouracil. The solution was saturated with dry HBr gas at 0 °C, sealed, and heated in an oil bath at 110 °C for 48 h. After cooling to room temperature, white precipitates were obtained upon adding petroether to the reaction solution. Recrystallization from acetone/petroether yielded 105 mg of [2-^{17}O]thymine (yield 62% based on thiouracil). The product was confirmed by ^1H and ^{13}C NMR spectra. Solution ^{17}O NMR indicated that ^{17}O labeling occurred primarily at the O2 position, $\delta(^{17}O) = 248$ ppm, with a small amount of [4-^{17}O]-thymine (<12%, $\delta(^{17}O) = 320$ ppm).

[4-^{17}O]Thymine. A mixture of 50 mg of thymine and 0.9 mL of $H_2{}^{17}O$ presaturated with dry HCl gas was sealed in a 1.0 mL glass vial with a Teflon/silicone septa. The reactor was placed in an oil bath (98−103 °C) for 21 h. After cooling to room temperature, the excessive labeled water was recovered on a vacuum line. The product was confirmed by ^1H and ^{13}C NMR. Solution ^{17}O NMR further confirmed the presence of ^{17}O labels only at the O4 position, $\delta(^{17}O) = 321$ ppm. The ^{17}O enrichment level of the sample is estimated to be less than 20%.

[4-^{17}O]Uracil. To 1.0 mL of $H_2{}^{17}O$ was added 90 mg of uracil. The solution was saturated with dry HCl gas, sealed, and kept stirring at 95 °C for 18 h. The purity of the product was confirmed by ^1H and ^{13}C NMR. The ^{17}O NMR spectrum of the compound in DMSO solution indicated that ^{17}O labeling occurred only at O4, $\delta(^{17}O) = 333.5$ ppm.

[2,4-^{17}O]Uracil. This compound was prepared in a similar fashion as that for [4-^{17}O]uracil, except that a much longer reaction time was used, ca. 9 days. At an acidic pH, two peaks were observed in the ^{17}O NMR spectrum of the compound, 227.3 and 288.0 ppm, which were assigned to O4 and O2, respectively. This is in agreement with a previous study.[3]

[2-^{17}O]Uracil. This compound was prepared by back exchange of [2,4-^{17}O]uracil in concentrated HCl aqueous solution containing unlabeled H_2O at 90 °C for 7 days. The ^{17}O back exchange process was monitored by solution ^{17}O NMR. The final ^{17}O NMR spectrum of the compound showed only one peak at 288 ppm (at an acidic pH) attributable to O2. It was noted that the loss of ^{17}O at the O2 position was negligible as compared with that of the starting compound, [2,4-^{17}O]uracil.

(14) (a) Samoson, A.; Lippmaa, E.; Pines, A. *Mol. Phys.* **1988**, *65*, 1013. (b) Chmelka, B. F.; Mueller, K. T.; Pines, A.; Stebbins, J.; Wu, Y.; Zwanziger, J. W. *Nature (London)* **1989**, *339*, 42. (c) Wu, Y.; Sun, B. Q.; Pines, A.; Samoson, A.; Lippmaa, E. *J. Magn. Reson.* **1990**, *89*, 297.
(15) (a) Frydman, L.; Harwood, J. S. *J. Am. Chem. Soc.* **1995**, *117*, 5367. (b) Medek, A.; Harwood, J. S.; Frydman, L. *J. Am. Chem. Soc.* **1995**, *117*, 12779.
(16) Wu, G.; Rovnyak, D.; Sun, B. Q.; Griffin, R. G. *Chem. Phys. Lett.* **1996**, *249*, 210.
(17) Wu, G.; Dong, S. *J. Am. Chem. Soc.* **2001**, *123*, 9119.
(18) Dong, S.; Yamada, K.; Wu, G. *Z. Naturforsch.* **2000**, *55A*, 21.
(19) Wu, G.; Hook, A.; Dong, S.; Yamada, K. *J. Phys. Chem. A.* **2000**, *104*, 4102.
(20) Wu, G.; Yamada, K.; Dong, S.; Grondey, H. *J. Am. Chem. Soc.* **2000**, *122*, 4215.
(21) Yamada, K.; Dong, S.; Wu, G. *J. Am. Chem. Soc.* **2000**, *122*, 11602.
(22) Dong, S.; Ida, R.; Wu, G. *J. Phys. Chem. A* **2000**, *104*, 11194.
(23) Wu, G.; Dong, S. *Chem. Phys. Lett.* **2001**, *334*, 265.
(24) Wu, G.; Dong, S.; Ida, R. *Chem. Commun.* **2001**, 891.
(25) Wang, S. Y.; Hahn, B. S.; Fenselau, C.; Zafiriou, O. C. *Biochem. Biophys. Res. Commun.* **1972**, *48*, 1630.
(26) Puzo, G.; Schram, K. H.; McCloskey, J. A. *Nucleic Acids Res.* **1977**, *4*, 2075.

[2-^{17}O]Cytosine. In $H_2{}^{17}O$ saturated with dry HCl gas in a 1.0 mL glass vial was dissolved 100 mg of 2-thiocytosine (0.79 mmol). The vial was then sealed and kept at 95−98 °C for 90 h. After recovery of $H_2{}^{17}O$ by high vacuum distillation, the chloride product was neutralized with an excess of ammonia solution and further purified by washing with water and recrystallizing from ethanol. The final yield was 52 mg (59%). Complete conversion of 2-thiocytosine to cytosine was confirmed by the disappearance of the 179 ppm peak (C═S) and the appearance of a new peak at 167 ppm (C═O) in ^{13}C NMR spectra. The ^{17}O NMR of the compound in DMSO and ammonia solution exhibits a peak at 245 ppm, whereas in DMSO and HCl solution the signal was changed to 264 ppm. The ^{17}O enrichment level of [2-^{17}O]-cytosine was 40%.

[6-^{17}O]Guanine·H_2O. To 1 mL of $H_2{}^{17}O$ saturated with dry HBr gas was added 100 mg of 6-thioguanine. The reaction vial was sealed and kept at 95−98 °C for 26 h. After removal of excessive $H_2{}^{17}O$ by high vacuum distillation, the bromide product was neutralized with excessive ammonia solution. The neutral product was further purified by recrystallization from ethanol. The total yield was 52 mg (59%). Complete conversion of 6-thioguanine to guanine was confirmed by the disappearance of the 172 ppm peak (C═S) and the appearance of a new peak at 156 ppm (C═O) in ^{13}C NMR spectra. The solution ^{17}O NMR spectrum of [6-^{17}O]guanine bromide showed a peak at 300.2 ppm, but in a neutral DMSO solution, the ^{17}O NMR signal of [6-^{17}O]-guanine appeared at 346 ppm, consistent with a previous study.[3] The ^{17}O enrichment level of [6-^{17}O]guanine was 40%.

Solid-State ^{17}O NMR. All solid-state ^{17}O NMR spectra were recorded on a Bruker Avance-500 spectrometer operating at 500.13 and 67.78 MHz for ^{1}H and ^{17}O nuclei, respectively. Polycrystalline samples were packed into zirconium oxide rotors (4 mm o.d.). A Bruker 4 mm MAS probe was used for ^{17}O static and MAS experiments. The B_1 field strength at the ^{17}O Larmor frequency was approximately 80 kHz. Sample spinning frequency in the MAS experiments was controlled at 14 500 ± 2 Hz. In the ^{17}O static experiments, the echo sequence proposed by Oldfield and co-workers[27] was used to avoid spectral distortion arising from acoustic ring-down of the probe. Typical recycle delays ranged from 5 to 10 s. Other experimental details are given in the figure captions. Spectral simulations were performed with the WSOLIDS program package (Klaus Eichele and Rod Wasylishen, Dalhousie University, Halifax, Canada).

Quantum Chemical Calculations. All quantum chemical calculations on ^{17}O EFG and chemical shielding (CS) tensors were carried out with the Gaussian98 suite of programs[28] on two Pentium personal computers (400 MHz, 128 MB of RAM, 20 GB of disk space; 800 MHz, 256 MB of RAM, 81.9 GB of disk space). The standard basis set of 6-311++G(d,p) and the B3LYP exchange functional[29] were employed. The gauge including atomic orbital (GIAO) approach[30] was used for chemical shielding calculations. Molecular cluster models were constructed using the experimental X-ray crystal structures.[31−34] Because X-ray diffraction studies did not produce accurate positions for hydrogen atoms, standard values for C−H (1.100 Å) and N−H (1.030 Å) bonds were used to generate hydrogen atoms in the theoretical models. Detailed discussion about the hydrogen-bonding geometry in the nucleobases will be presented in the following sections. It should be mentioned that, with our limited computing resources, long computational times were generally required for the quantum chemical calculations reported in this study. Typically, GIAO chemical shielding calculations need several hours of CPU time for isolated molecules and several days for large molecular clusters. To make direct comparison between the calculated chemical shielding, σ, and the observed chemical shift, δ, we used the absolute ^{17}O chemical shielding scale established by Wasylishen and co-workers:[35]

$$\delta = 307.9 \text{ ppm} - \sigma \qquad (1)$$

Alternatively, one can combine a calculated ^{17}O shielding value of 326 ppm for gaseous H_2O with the experimental gas-to-liquid shift of 36 ppm to convert absolute shielding values to chemical shifts. This approach will generate a systematic discrepancy of 54 ppm for all data, as compared to the method of eq 1. For the quadrupole interaction, since the quantum chemical calculations yield EFG tensor components, $q_{ii,}$ in atomic unit (au), the following equation was used to convert them to the quadrupolar coupling constant (QCC), C_Q, in MHz:

$$C_Q[\text{MHz}] = e^2Qq_{zz}h^{-1} = -2.3496Q[\text{fm}^2]q_{zz}[\text{au}] \qquad (2)$$

where Q is the nuclear quadrupole moment of the ^{17}O nucleus (in fm^2), and the factor of 2.3496 results from unit conversion. In the present study, we use $Q(^{17}\text{O}) = -2.330$ fm^2, which was previously calibrated for the B3LYP/6-311++G(d,p) level of calculations.[21] Another important parameter is known as the asymmetry parameter (η_Q): $\eta_Q = (q_{xx} - q_{yy})/q_{zz}$.

3. Results and Discussion

Spectral Analyses. Since ^{17}O is a half-integer quadrupolar nucleus ($I = {}^5/_2$), spectral analysis of solid-state NMR spectra is more complex than that for spin-$^1/_2$ nuclei. In general, for a half-integer quadrupolar nucleus in a strong magnetic field, one needs to consider only the central transition ($+{}^1/_2 \leftrightarrow -{}^1/_2$). Under such a circumstance, both chemical shift anisotropy and second-order quadrupole interactions manifest themselves in the NMR spectra. To obtain information about these two types of NMR tensors, one usually performs NMR experiments under two different conditions: MAS and static. Because the second-order quadrupole interaction is not averaged to zero by MAS, three spectral parameters can be obtained from an analysis of MAS spectra: isotropic chemical shift (δ_{iso}), C_Q, and η_Q. It is important to note that the sign of C_Q is not obtainable from ^{17}O MAS spectra. In the present study, we relied on the quantum chemical calculations to determine the sign of C_Q. From the static spectra, one can obtain values of the chemical shielding tensor components and their relative orientation with respect to the EFG tensor. A detailed theory for solid-state ^{17}O NMR spectral analysis has been given in a previous study.[21]

Figure 1 shows the experimental and simulated ^{17}O MAS spectra for compounds **1**−**6**. Each of the ^{17}O MAS spectra exhibits a typical line shape arising from the second-order quadrupole interaction. The observed line width is on the order of 10 kHz, indicating the presence of sizable ^{17}O quadrupole

(27) Kunwar, A. C.; Turner, G. L.; Oldfield, E. *J. Magn. Reson.* **1986**, *69*, 124.
(28) Frisch, M. J.; Trucks, G. W.; Schlegel, H. B.; Scuseria, G. E.; Robb, M. A.; Cheeseman, J. R.; Zakrzewski, V. G.; Montgomery, J. A., Jr.; Stratmann, R. E.; Burant, J. C.; Dapprich, S.; Millam, J. M.; Daniels, A. D.; Kudin, K. N.; Strain, M. C.; Farkas, O.; Tomasi, J.; Barone, V.; Cossi, M.; Cammi, R.; Mennucci, B.; Pomelli, C.; Adamo, C.; Clifford, S.; Ochterski, J.; Petersson, G. A.; Ayala, P. Y.; Cui, Q.; Morokuma, K.; Malick, D. K.; Rabuck, A. D.; Raghavachari, K.; Foresman, J. B.; Cioslowski, J.; Ortiz, J. V.; Stefanov, B. B.; Liu, G.; Liashenko, A.; Piskorz, P.; Komaromi, I.; Gomperts, R.; Martin, R. L.; Fox, D. J.; Keith, T.; Al-Laham, M. A.; Peng, C. Y.; Nanayakkara, A.; Gonzalez, C.; Challacombe, M.; Gill, P. M. W.; Johnson, B. G.; Chen, W.; Wong, M. W.; Andres, J. L.; Head-Gordon, M.; Replogle, E. S.; Pople, J. A. *Gaussian 98*, revision A.6; Gaussian, Inc.: Pittsburgh, PA, 1998.
(29) (a) Becke, A. D. *Phys. Rev.* **1988**, *A38*, 3098. (b) Lee, C.; Yang, W.; Parr, R. G. *Phys. Rev.* **1988**, *B37*, 785. (c) Becke, A. D. *J. Chem. Phys.* **1993**, *98*, 5648.
(30) (a) Ditchfield, R. *Mol. Phys.* **1974**, *27*, 789. (b) Wolinski, K.; Hilton, J. F.; Pulay, P. *J. Am. Chem. Soc.* **1990**, *112*, 8257.
(31) Ozeki, K.; Sakabe, N.; Tanaka, J. *Acta Crystallogr.* **1969**, *B25*, 1038.
(32) Stewart, R. F. *Acta Crystallogr.* **1967**, *23*, 1102.
(33) (a) Barker, D. L.; Marsh, R. E. *Acta Crystallogr.* **1964**, *17*, 1581. (b) McClure, R. J.; Craven, B. M. *Acta Crystallogr.* **1973**, *B29*, 1234.
(34) Thewalt, U.; Bugg, C. E.; Marsh, R. E. *Acta Crystallogr.* **1971**, *B27*, 2358.
(35) Wasylishen, R. E.; Mooibroek, S.; Macdonald, J. B. *J. Chem. Phys.* **1984**, *81*, 1057.

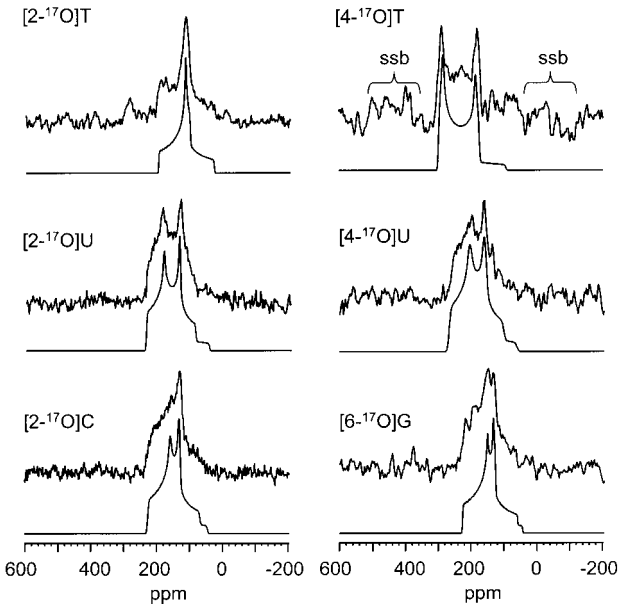

Figure 1. Experimental (upper trace) and simulated (lower trace) ^{17}O MAS NMR spectra of free nucleic acid bases at 11.75 T. Chemical shifts are referenced to liquid H_2O. The number of scans (NS) and recycle delay (RD) are given below. [2-^{17}O]T: NS, 3753; RD, 10 s. [4-^{17}O]T: NS, 5236; RD, 10 s. [2-^{17}O]U: NS, 1273; RD, 5 s. [4-^{17}O]U: NS, 1228; RD, 10 s. [2-^{17}O]C: NS, 4550; RD, 10 s. [6-^{17}O]G: NS, 7195; RD, 10 s.

couplings. Because of the limitation in both ^{17}O enrichment and quantity of samples, the overall signal-to-noise (S/N) ratio in the ^{17}O NMR spectra shown in Figure 1 is rather low. Nevertheless, it is possible to analyze these MAS spectra and obtain reliable ^{17}O NMR parameters. At the present S/N levels, we estimate the accuracy in δ_{iso}, C_Q, and η_Q to be ± 5 ppm, ± 0.05 MHz, and $\pm$ 0.05, respectively. This means that simulations with parameters outside these ranges would produce noticeable discrepancies between the observed and calculated spectra. To obtain information about the ^{17}O chemical shielding tensor, it is necessary to obtain static ^{17}O NMR spectra. As seen from Figure 2, the experimental ^{17}O NMR spectra for stationary samples generally cover a large frequency range (ca. 30−60 kHz). Each spectrum exhibits several singularities either as peaks or as steps. These spectral features are known as the critical frequencies or critical points.[36] Following the procedure outlined in our previous study,[21] we obtained the ^{17}O chemical shielding tensor components and their relative orientations. Again, at the present level of S/N, the accuracy in the tensor components and the Euler angles was estimated to be ± 10 ppm and $\pm$ 5°, respectively. Experimental solid-state ^{17}O NMR results are summarized in Table 1. To aid the following discussion, a brief summary of the crystal structures for the four nucleobases investigated in the present study is given in Table 2.

Thymine. Thymine crystallizes in the space group $P2_1/c$.[31] The two oxygen atoms of the thymine molecule, O2 and O4, are related to the urea- and amide-type functional group, respectively. In the crystal lattice, thymine molecules are linked through C═O···H−N hydrogen bonds. As seen from Figure 3, whereas O2 is directly involved in two hydrogen bonds (O···N = 2.816 and 2.836 Å), O4 is free of any hydrogen-bonding interaction. The strong hydrogen bonding at O2 is also responsible for the rather long C═O bond length at O2 (1.246 Å). In comparison, the C═O bond length at O4 is only 1.193 Å. As a result of these structural differences, O2 and O4 of thymine exhibit drastically different ^{17}O NMR tensors; see Table 1. In particular, the amide-type oxygen, O4, shows a much larger C_Q, 8.40 MHz, than that of the urea-type oxygen, O2, 6.65 MHz. It is noted that the C_Q value for O2 is even smaller than that found in crystalline urea, 7.24 MHz.[22] The difference between the ^{17}O CS tensors for O2 and O4 is also striking. The isotropic ^{17}O chemical shifts for O2 and O4 differ by 125 ppm. Furthermore, the span ($\Omega = \delta_{11} - \delta_{33}$) of the ^{17}O CS tensor for O4 is more than twice that for O2. These observations are in agreement with the general trend found for the ^{17}O NMR parameters in carbonyl compounds.

Uracil. In contrast to the crystal packing in thymine, the hydrogen bonding in uracil crystals involves only the amide-type oxygen atom, O4, whereas O2 is free of intermolecular interactions.[32] Once again, we note that the oxygen atom involved in strong hydrogen bonding gives rise to a longer C═O bond (1.215 and 1.245 Å for O2 and O4, respectively). The two O···N hydrogen bonds centered at O4 are similar in length, 2.864 and 2.865 Å. It is interesting that O2 and O4 exhibit somewhat similar C_Q values, 7.61 and 7.85 MHz, despite the fact that the two oxygen atoms belong to quite different functional groups. The explanation for this observation is that there are two competing factors that determine the magnitude of C_Q for amide and urea functional groups. First, amide groups generally exhibit larger ^{17}O C_Q values than those of urea-type groups.[20−22] Second, direct involvement in hydrogen bonding tends to reduce the size of C_Q at the oxygen atom. The competition between these two factors can be best illustrated with the ^{17}O NMR data observed for thymine and uracil. In crystalline thymine, the urea-type oxygen is involved in strong hydrogen bonding. Therefore, the observed difference between C_Q values for O2 and O4 is very large. In crystalline uracil, however, the fact that the amide oxygen is involved in strong hydrogen bonding makes the C_Q value for O4 smaller, that is, more similar to the C_Q value of O2. Similar competing factors are also operative in determining the ^{17}O chemical shielding environment. As mentioned earlier, the observed isotropic ^{17}O chemical shift difference between O2 and O4 of thymine is very large, 125 ppm. In contrast, the chemical shift difference between O2 and O4 of uracil is only 30 ppm. Again, this is because the hydrogen-bonding arrangement between the amide- and urea-type oxygen atoms in uracil crystals is opposite to that in thymine.

Cytosine. Unlike thymine and uracil, cytosine crystals exhibit a different packing motif. In particular, the cytosine molecules are linked by hydrogen bonds (N−H···O═C and N−H···N) to form ribbons along the *b* direction, but the ribbons are tilted about 27.5° from parallel to the *ab* plane.[33] As is evident from Figure 3, the cluster structure of cytosine is nonplanar. The O2 atom is directly involved in two hydrogen bonds (O···N, 2.98 and 3.03 Å). These hydrogen bonds are considerably longer than those found in thymine and uracil crystals. In cytosine, the C═O bond length, 1.241 Å, is significantly longer than the C═O bond for O2 of uracil (1.215 Å), but very similar to that for O2 of thymine (1.246 Å). This suggests that in cytosine the hydrogen-bonding interaction at O2 is also strong. The observed C_Q for cytosine, 7.20 MHz, is consistent with the prediction based on the C═O bond length. Similarly, the ^{17}O chemical

(36) Chu, P.-J.; Gerstein, B. C. *J. Chem. Phys.* **1989**, *91*, 2081.

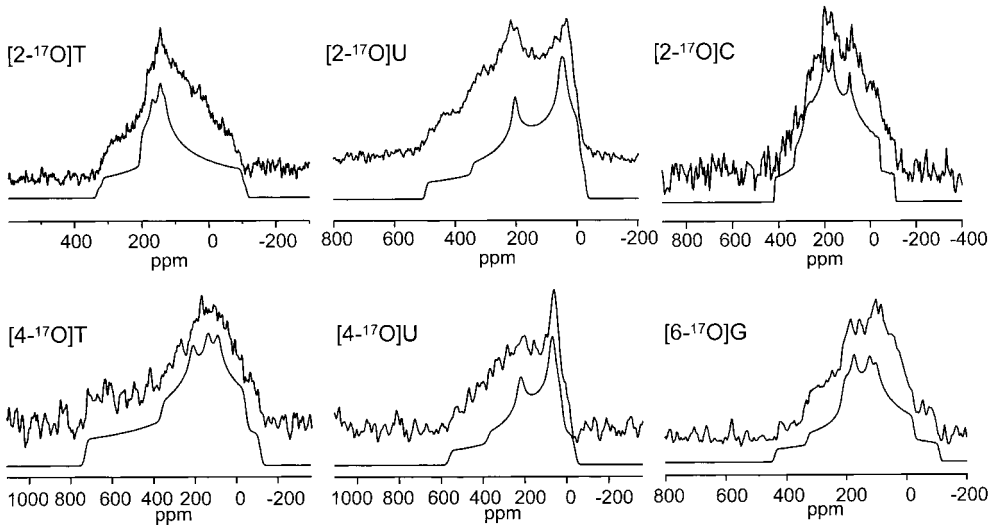

Figure 2. Experimental (upper) and simulated (lower) ^{17}O static NMR spectra of free nucleic acid bases at 11.75 T. Chemical shifts are referenced to liquid H_2O. The number of scans (NS) and recycle delay (RD) are given below. [2-^{17}O]T: NS, 7400; RD, 10 s. [4-^{17}O]T: NS, 8462; RD, 10 s. [2-^{17}O]U: NS, 4277; RD, 5 s. [4-^{17}O]U: NS, 5287; RD, 10 s. [2-^{17}O]C: NS, 8271; RD, 10 s. [6-^{17}O]G: NS, 15 765; RD, 5 s.

Table 1. Experimental Solid-State ^{17}O NMR Results for Free Nucleic Acid Bases[a]

compound	δ_{liquid} /ppm	δ_{iso} /ppm	δ_{11} /ppm	δ_{22} /ppm	δ_{33} /ppm	C_Q /MHz	η_Q	α /deg	β /deg	γ /deg
[2-^{17}O]thymine	248	200	290	270	20	6.65	1.00	4	90	70
[4-^{17}O]thymine	321	325	570	360	20	8.40	0.10	0	84	84
[2-^{17}O]uracil	247	245	400	330	10	7.61	0.50	0	89	82
[4-^{17}O]uracil	329	275	470	350	10	7.85	0.55	0	90	75
[2-^{17}O]cytosine	245	230	350	300	40	7.20	0.70	12	80	70
[6-^{17}O]guanine	346	230	395	285	10	7.10	0.80	5	87	67

[a] Chemical shifts (δ_{liquid}) were measured in DMSO solution and referenced to liquid H_2O. Errors in the experimental isotropic chemical shifts and principal tensor components are ±5 and ±10 ppm, respectively. Errors in the experimental quadrupole coupling constants and asymmetry parameters are 0.05 MHz and 0.05, respectively. Errors in the Euler angles are ±5°.

Table 2. Summary of Crystal Structure Data for the Free Nucleic Acid Bases

compound	crystal form	space group		r(C═O) /Å	hydrogen bonding	ref
thymine	monoclinic	$P2_1/c$	O2	1.246	O···N (2.810 Å)	31
					O···N (2.836 Å)	
			O4	1.193	none	
uracil	monoclinic	$P2_1/a$	O2	1.215	none	32
			O4	1.245	O···N (2.864 Å)	
					O···N (2.865 Å)	
cytosine	orthorhombic	$P2_12_12_1$	O2	1.241	O···N (2.98 Å)	33
					O···N (3.03 Å)	
guanine	monoclinic	$P2_1/n$	O6	1.239	O···N (2.93 Å)	34
					O···O (2.71 Å)	

shift value observed for O2 of cytosine, 230 ppm, is also between those for the O2 groups of thymine (200 ppm) and uracil (245 ppm). This suggests that there exists a parallelism between ^{17}O quadrupole couplings and chemical shifts (vide infra).

Guanine. As the only purine base examined in this study, guanine exhibits some unique features. The guanine molecules are connected by N−H···O (2.93 Å) and N−H···N (2.83 Å) hydrogen bonds in a zigzag fashion;[34] see Figure 3. The oxygen atom, O6, also forms an O···H−O hydrogen bond (2.71 Å) to a water molecule. In addition, each water molecule also accepts a hydrogen bond from an $-NH_2$ group. The guanine molecule is essentially planar and adopts the tautomeric form where the nitrogen atom, N(1), is protonated. The C═O bond length at O6, 1.239 Å, is similar to those found for the C═O groups

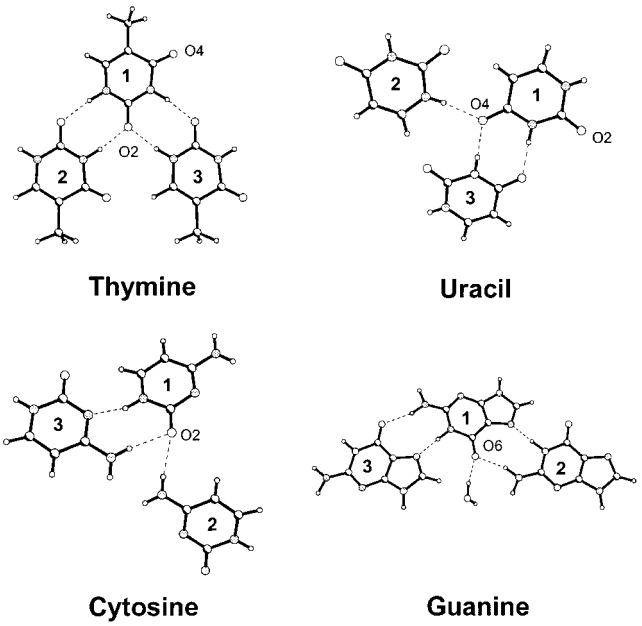

Figure 3. Molecular cluster models constructed from experimental X-ray crystal structures. See text for detailed discussion.

involved in strong hydrogen bonding, for example, O2 of thymine and O4 of uracil. However, it is interesting to note that, although the carbonyl group at O6 is similar to an amide group, the observed ^{17}O NMR parameters for [6-^{17}O]guanine (C_Q = 7.10 MHz and δ_{iso} = 230 ppm) are more consistent with

Table 3. Calculated B3LYP/6-311++G(d,p) ^{17}O NMR Tensors for Free Nucleic Acid Bases[a]

compound	model	δ_{iso} /ppm	δ_{11} /ppm	δ_{22} /ppm	δ_{33} /ppm	C_Q /MHz	η_Q	compound	model	δ_{iso} /ppm	δ_{11} /ppm	δ_{22} /ppm	δ_{33} /ppm	C_Q /MHz	η_Q
[2-^{17}O]thymine	opt[b]	300	459	410	30	7.762	0.366	[4-^{17}O]uracil	opt	407	708	505	8	8.945	0.017
	I	295	441	406	48	8.424	0.551		I	423	747	521	−1	9.684	0.116
	II	264	385	359	46	7.817	0.735		II	384	670	479	1	9.195	0.221
	III	250	365	344	40	7.721	0.792		III	372	647	466	1	9.110	0.257
	IV	226	327	306	45	7.125	0.990		IV	340	584	430	6	8.644	0.364
[4-^{17}O]thymine	opt	401	717	496	−9	8.929	0.019	[2-^{17}O]cytosine	opt	338	516	451	46	8.302	0.201
	I	387	698	487	−25	8.908	0.140		I	347	529	466	47	8.936	0.294
	II	380	685	480	−25	9.144	0.170		II	322	478	438	52	8.576	0.402
	III	399	734	496	−33	8.829	0.121		III	302	456	409	42	8.334	0.449
	IV	392	720	491	−34	9.077	0.150		IV	282	416	384	46	8.036	0.550
[2-^{17}O]uracil	opt	306	468	418	31	7.838	0.331	[6-^{17}O]guanine·H_2O	opt	354	606	469	−13	8.375	0.126
	I	308	493	427	4	8.306	0.282		I	360	625	471	−16	9.035	0.239
	II	314	510	433	−1	8.475	0.251		II	337	577	444	−11	8.863	0.304
	III	311	496	431	4	8.323	0.277		III	305	510	402	2	8.168	0.466
	IV	310	513	436	0	8.492	0.251		IV	275	468	368	−11	7.924	0.548

[a] Calculated chemical shifts were converted from the computed shielding values using eq1. [b] Optimized at the B3LYP/6-311G(d,p) level of theory.

those for a urea-type functional group accepting two hydrogen bonds such as the O2 atoms in thymine and cytosine. Clearly, the water molecule is a strong hydrogen-bond donor, which may contribute significantly to the small values of C_Q and δ_{iso}. Meanwhile, the difference between purine and pyrimidine groups further complicates any direct comparison of the ^{17}O NMR parameters between guanine and other base molecules. Nevertheless, it is important to point out that, due to the complex nature of the origin of NMR parameters, neither the C═O bond length nor the hydrogen bonding alone can provide an adequate explanation of the observed trends in the ^{17}O NMR tensors. Further work is clearly needed to provide a unified theory for interpreting ^{17}O NMR tensors in all carbonyl compounds.

Comparison between Experimental and Theoretical ^{17}O NMR Tensors. To better understand the observed ^{17}O NMR tensors described in previous sections, we decided to perform quantum chemical calculations for the ^{17}O EFG and CS tensors in nucleobase systems. The primary objective of the theoretical work is 2-fold. First, our previous studies on amides have indicated that it is necessary to include a complete hydrogen-bonding network in the theoretical model.[20,21] However, it is uncertain whether the same conclusion is valid for heterocyclic bases where the hydrogen-bonding geometry is often planar. Second, since we have obtained the first set of experimental ^{17}O NMR data for nucleobases, it is hoped that comparison between experimental and computational results may shed light on the relationship between ^{17}O NMR tensors and structural features. It is obviously important to address these questions before solid-state ^{17}O NMR can be used as a probe to base pairing in nucleic acids.

To evaluate quantitatively the influence of intermolecular hydrogen-bonding interactions on the ^{17}O EFG and CS tensors in nucleobases, we selected several models for quantum chemical calculations. First, we obtained the fully optimized structure for each base molecule at the B3LYP/6-311G(d,p) level of theory. Second, four additional models were constructed using experimental X-ray diffraction structures.[31−34] In particular, Model-I is simply an isolated molecule. For the pyrimidine bases (thymine, uracil, and cytosine), Model-II consists of two hydrogen-bonded molecules, Mol1 and Mol2, as defined in Figure 3. Model-III also consists of two molecules, Mol1 and Mol3. Model-IV is a trimeric cluster containing Mol1, Mol2, and Mol3. For the purine base (i.e., guanine monohydrate), Model-II consists of Mol1 and the water molecule. In Model-III, Mol2 is added to the cluster of Model-II. Finally, Model-IV contains three guanine molecules and a water molecule. The computed ^{17}O NMR tensors for the nucleobases are presented in Table 3.

From the theoretical results presented in Table 3, several general trends are observed. First, for the oxygen atoms involved in strong hydrogen bonding, both EFG and CS results depend strongly on the cluster model used in the calculation. For example, Model-I of thymine predicts $\delta_{iso} = 295$ ppm and $C_Q = 8.424$ MHz for O2, whereas Model-IV yields $\delta_{iso} = 226$ ppm and $C_Q = 7.125$ MHz. The same trend is also evident in the results for O4 of uracil, O2 of cytosine, and O6 of guanine. However, for the oxygen atoms that are not directly involved in any hydrogen bonding, EFG and CS results are approximately independent of the model. For instance, the calculated values of δ_{iso} and C_Q for O4 of thymine from Model-I and Model-IV differ by only 5 ppm and 0.069 MHz, respectively. This is a clear indication that ^{17}O NMR tensors are highly sensitive to hydrogen bonding. Interestingly, as compared with previous results on secondary amides,[21] the ^{17}O NMR tensors in nucleobases exhibit a considerably greater sensitivity to the cluster size, indicating that the hydrogen bonding is much stronger in nucleobases than in amides. Among the four nucleobases examined in the present study, the largest ^{17}O chemical shift changes from Model-I to Model-IV occur at O4 of uracil and O6 of guanine, 83 and 85 ppm, respectively. Accordingly, the changes in C_Q for these groups are also very large, 1.040 and 1.111 MHz. Intermolecular effects of similar magnitude have only been observed in benzamide[20] and urea.[22] For benzamide, it is known that the formation of a cyclic dimer held by two hydrogen bonds plays an important role in enhancing the hydrogen-bonding effect. Meanwhile, urea represents a unique example where the carbonyl oxygen atom accepts four direct hydrogen bonds. Our calculations show that the hydrogen bonding in the free nucleic acid bases also belongs to this class of systems where hydrogen bonding is reinforced by the molecular structure. In both α-helix and β-sheet structures of peptides, the carbonyl oxygen atom is usually involved in only one C═O···H−N hydrogen bond, whereas in base pairing, the hydrogen bonds are arranged in a cyclic fashion. This may suggest that ^{17}O NMR may be more useful in detecting base pairing in nucleic acids than detecting structures of proteins.

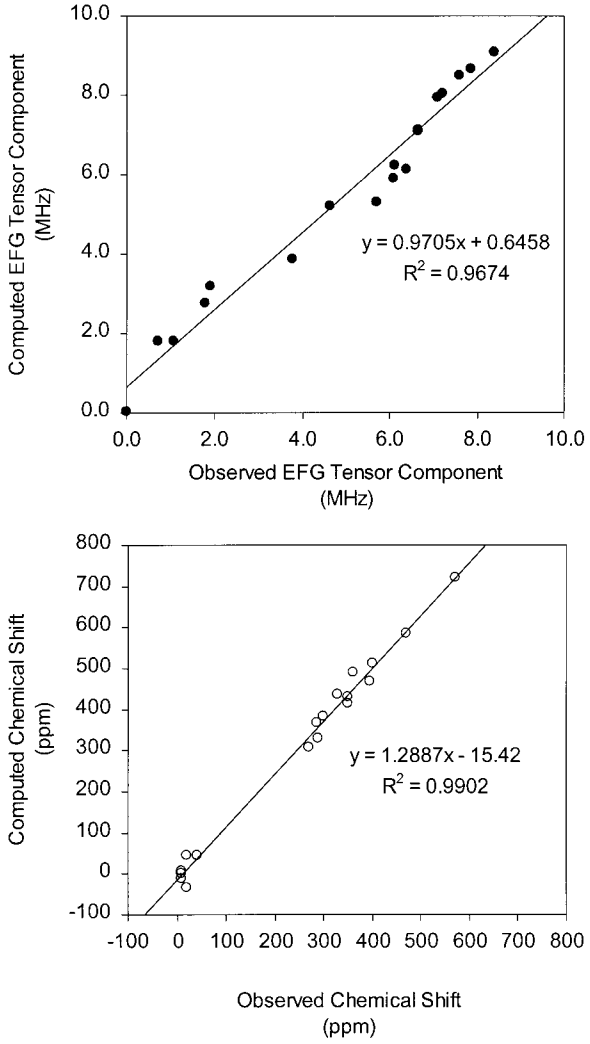

Figure 4. Comparison between the experimental and theoretical ^{17}O EFG tensors (top) and chemical shift tensors (bottom) for nucleobases. The calculated chemical shifts are converted from the computed shielding values using eq 1. The EFG tensor components are expressed in units of MHz using eq 2. Here the absolute values of the EFG tensor components are plotted.

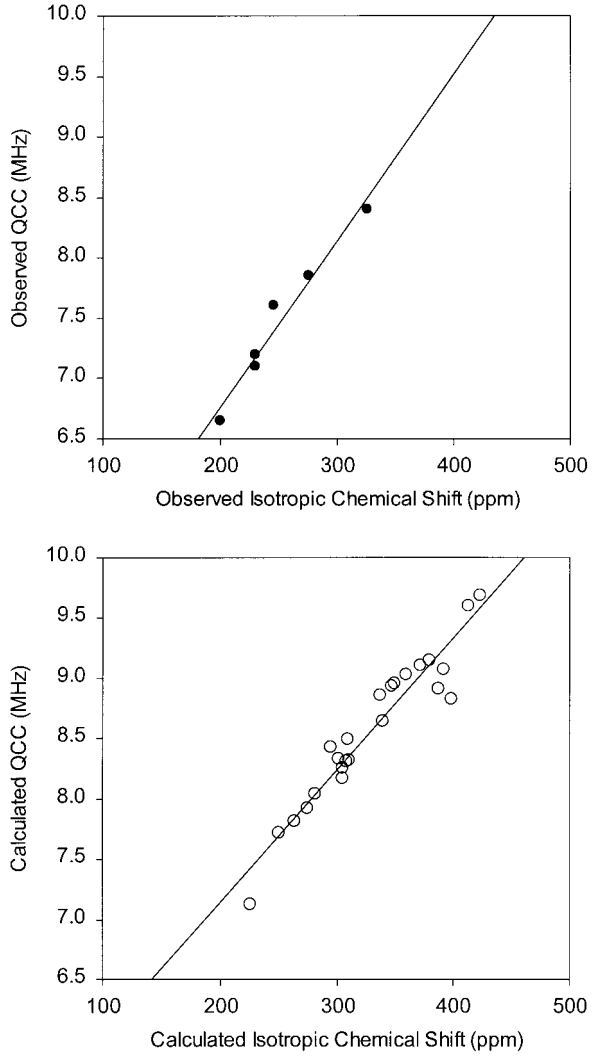

Figure 5. The correlation between the ^{17}O quadrupole coupling constant and the ^{17}O isotropic chemical shift. Top: experimental data. Bottom: theoretical data.

Second, it can be seen from Table 3 that the CS tensor components show even larger variations among different models than do the isotropic chemical shifts. For example, the difference between the δ_{11} components in Model-I and Model-IV for guanine is 157 ppm, which is approximately twice as large as the change of the isotropic chemical shifts, 85 ppm. In addition, only changes in δ_{11} and δ_{22} components are responsible for the observed decrease in the isotropic ^{17}O chemical shift (increase in *shielding*) from Model-I to Model-IV. Third, as shown in Figure 4, the calculated results from Model-IV are in reasonably good agreement with the experimental data. Clearly, inclusion of several immediate neighbor molecules in the theoretical model can reproduce, to a very good degree of accuracy, the ^{17}O EFG properties in the crystal lattice. It is also noted that the B3LYP/6-311++G(d,p) calculations overestimate the paramagnetic shielding by approximately 30% in a fairly uniform fashion across a range of 600 ppm.

Correlations between ^{17}O NMR Parameters. In the above discussion, we have noticed an apparent parallelism between the ^{17}O quadrupole coupling constant and the isotropic chemical shift. As shown in Figure 5, a nice correlation is indeed observed between these two fundamental NMR parameters. The experimental ^{17}O NMR data observed for nucleobases span approximately 120 ppm for δ_{iso} and 2 MHz for C_Q, reflecting large variations in the chemical bonding among the four nucleobases. In fact, a similar correlation exists among all carbonyl compounds ranging from aldehydes to amides.[37] As also seen in Figure 5, the experimental correlation is very well reproduced by the quantum chemical calculations. The two slopes in Figure 5 are essentially the same. It should be noted that the theoretical data presented in Figure 5 contain results from all cluster models (Model-I through Model-IV) for each of the bases. Even though the two types of nuclear magnetic properties have fundamentally different origins, this correlation implies that the two NMR quantities are also intrinsically connected and that it may be redundant to obtain both types of NMR tensors for a series of closely related compounds. Interestingly, similar correlations between C_Q and δ_{iso} have been previously observed for ^{59}Co and ^{17}O nuclei.[38−40]

(37) Yamada, K.; Wu, G. 42nd Experimental NMR Conference, Poster # W&TH P217, Orlando, Florida, March 11−16, 2001, and unpublished results.

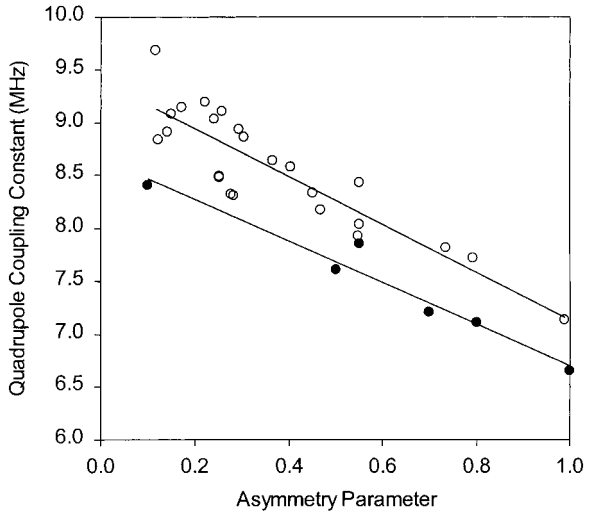

Figure 6. The correlation between the experimental (filled circles) and calculated (open circles) ^{17}O quadrupole coupling constants and asymmetry parameters for nucleobases.

It is worth commenting on another type of correlation that is apparent from the data in Tables 1 and 3. As shown in Figure 6, a clear correlation is found between the ^{17}O quadrupole coupling constant and the corresponding asymmetry parameter for nucleobases. The general trend is that η_Q increases monotonically with a decrease of C_Q. Since the value of C_Q depends strongly on the strength of hydrogen bonding, it is evident that η_Q can also be used as an indicator of hydrogen bonding. This type of correlation was first discovered from ^{17}O NQR data.[41] As also seen from Figure 6, the theoretical data lie slightly above the experimental data, suggesting that calculations at the B3LYP/6-311++G(d,p) level of theory overestimate the ^{17}O quadrupole coupling constant by approximately 5%.

Orientations of the ^{17}O EFG and CS Tensors. As indicated in Table 1, an important piece of information from the analyses of solid-state ^{17}O NMR spectra is the *relative* orientation between the ^{17}O EFG and CS tensors. However, tensor orientations in the molecular frame are still unknown. In the absence of single-crystal ^{17}O NMR data, high-level quantum chemical calculations have proven to be a viable approach for obtaining information about NMR tensor orientations in the molecular frame. Recent work from this laboratory has produced benchmark values for the accuracy of both ^{17}O EFG and CS tensors in hydrogen-bonded systems.[19−22,24] We have concluded that quantum chemical calculations at the B3LYP/6-311++G(d,p) level of theory can produce reliable results for NMR tensor orientations, although the magnitude of individual tensor components computed at this level is of lesser accuracy. In the present case, nucleic acid bases represent another opportunity to further examine the validity of quantum chemical calculations for ^{17}O NMR tensors in solid samples. It should be noted that, among the very few theoretical studies on nucleobases available in the literature, contradicting results existed regarding the

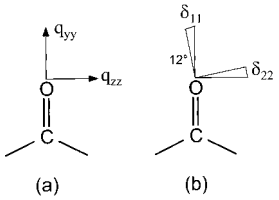

Figure 7. The orientations of the ^{17}O EFG and chemical shift tensors in the molecular frame. Both q_{xx} and δ_{33} are perpendicular to the molecular plane.

orientation of the ^{17}O CS tensor in the molecular frame. For example, Giessner-Prettre and co-workers[42] calculated the ^{17}O CS tensor for cytosine. Their results suggested that the tensor component with the least shielding, δ_{11}, lies close to the C═O bond direction. However, in a later comprehensive IGLO evaluation of the NMR tensors for nucleobases, Schindler[43] reported that this tensor component is perpendicular to the C═O bond for all the urea-type oxygen atoms in cytosine, thymine, and uracil. It should be noted that neither Giessner-Prettre and co-workers nor Schindler considered the influence of hydrogen-bonding interactions. Recently, we reported a preliminary solid-state ^{17}O NMR study for crystalline thymine, which confirmed the conclusion by Giessner-Prettre and co-workers.[42] Here we further examine the ^{17}O NMR tensors in other nucleobases.

The calculated orientations for the ^{17}O EFG and CS tensors are depicted in Figure 7. For all the carbonyl oxygen atoms in the base molecules, the orientation of the ^{17}O EFG tensor was found to be essentially the same with respect to the C═O bond. That is, the largest component of the EFG tensor, q_{zz}, always lies in the molecular plane and is perpendicular to the C═O bond; meanwhile, the smallest component, q_{xx}, is perpendicular to the molecular plane. A unique case is that of [2-^{17}O]thymine where the EFG tensor is axially symmetric; that is, $q_{yy} = q_{zz}$. Similarly, variations of the ^{17}O CS tensor orientations are also insignificant between the amide- and urea-type oxygen groups. The tensor principal tensor component with the most shielding, δ_{33}, is invariantly perpendicular to the molecular plane. The component associated with the least shielding, δ_{11}, lies in the molecular plane deviating from the C═O bond by 0−12°. This general ^{17}O CS tensor orientation is in agreement with the results for other carbonyl compounds such as amides,[20,21,23] formaldehyde,[44] and benzophenone.[45] The relative orientation between the ^{17}O EFG and CS tensors shown in Figure 7 is also in excellent agreement with the experimental determination reported in Table 1.

G- and U-Quartet Structures. In this section, we attempt to evaluate the ^{17}O NMR tensors in two unusual structures: G- and U-quartets. The G-quartet structure consists of a tetrameric arrangement of quanine molecules. The G-quartet structure was first proposed by Gellert and co-workers to explain the fiber X-ray diffraction results for guanosine monophosphate (GMP) gels.[46] Subsequently, G-quartet structures have been observed in many systems.[47] The U-quartet structure was first observed

(38) Chung, S. C.; Chan, J. C. C.; Au-Yeung, S. C. F.; Xu, X. *J. Phys. Chem.* **1993**, *97*, 12685.
(39) Park, K. D.; Guo, K.; Adebodun, F.; Chiu, M. L.; Sligar, S. G.; Oldfield, E. *Biochemistry* **1991**, *30*, 2333.
(40) Ropp, J.; Lawrence, C.; Farrar, T. C.; Skinner, J. L. *J. Am. Chem. Soc.* **2001**, *123*, 8047.
(41) (a) Poplett, I. J. F.; Smith, J. A. S. *J. Chem. Soc., Faraday Trans. 2* **1979**, *75*, 1703. (b) Poplett, I. J. F.; Smith, J. A. S. *J. Chem. Soc., Faraday Trans. 2* **1981**, *77*, 1473. (c) Gready, J. E. *J. Am. Chem. Soc.* **1981**, *103*, 3682.
(42) (a) Prado, F. R.; Giessner-Prettre, C. *J. Magn. Reson.* **1982**, *47*, 103. (b) Giessner-Prettre, C.; Pullman, B. *J. Am. Chem. Soc.* **1982**, *104*, 70.
(43) Schindler, M. *J. Am. Chem. Soc.* **1988**, *110*, 6623.
(44) Gierke, T. D.; Flygare, W. H. *J. Am. Chem. Soc.* **1972**, *94*, 7277.
(45) Scheubel, W.; Zimmermann, H.; Haeberlen, U. *J. Magn. Reson.* **1985**, *63*, 544.
(46) Gellert, M.; Lipsett, M. N.; Davies, D. R. *Proc. Natl. Acad. Sci. U.S.A.* **1962**, *48*, 2013.

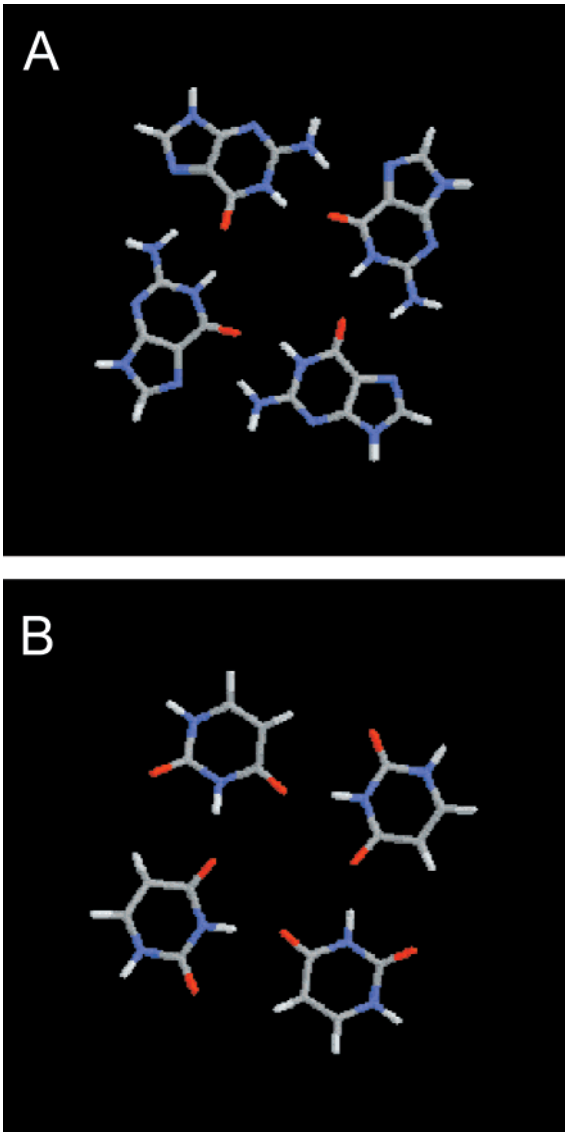

Figure 8. The G-quartet (top) and U-quartet (bottom) structures optimized at the B3LYP/6-311+G(d,p) level of theory (as reported by Meyer et al.[49]).

in an RNA tetraplex, $[r(UG_4U)]_4$, by Cheong and Moore[48] and is not as common as the G-quartet structures. As shown in Figure 8, both G- and U-quartet structures are held by cyclic C═O···H−N hydrogen bonds. These structural features are very different from those shown in Figure 3. Recently, Meyer et al.[49] reported fully optimized G- and U-quartet structures at the B3LYP/6-311+G(d,p) level of theory (Table 4). Using their structural data, we were able to calculate the ^{17}O NMR tensors in these unusual hydrogen-bond structures.

As seen from Figure 8, the target oxygen atom, O4, of the G-quartet is involved in only one hydrogen bond with an O4···H1 distance of 1.791 Å. The calculated ^{17}O data for the G-quartet are comparable to those from Models III of guanine monohydrate. For the U-qaurtet structure, the calculated ^{17}O NMR results are quite different from those for uracil crystals.

Table 4. Calculated B3LYP/6-311++G(d,p) ^{17}O NMR Tensors for G- and U-Quartet Structures[a]

	G-quartet	U-quartet	
E^b	−2170.91404	−1659.82667	
r(O4···H1)/Å	1.791	1.795	
r(O4···O4′)/Å[c]	4.993	5.041	
C_Q/MHz	8.087	O2: 9.034	O4: 7.990
η_Q	0.309	0.170	0.353
δ_{iso}/ppm[d]	317	379	294
δ_{11}/ppm	539	655	457
δ_{22}/ppm	412	463	401
δ_{33}/ppm	−1	21	25

[a] Both structures are optimized at the B3LYP/6-311+G(d,p) level theory with a C_{4h} symmetry. Data obtained from ref 49. [b]Total energy in kcal/mol. [c]Distance between O4 atoms at the opposite corners of the cavity. [d]Calculated chemical shifts were converted from the computed shielding values using eq 1.

In particular, C_Q and δ_{iso} for O4 are significantly smaller than the corresponding values found for uracil, suggesting that the cyclic formation in U-quartet represents a hydrogen-bonding environment stronger than the sum of two hydrogen bonds in uracil crystals. It is interesting to note that, for the oxygen atom free of hydrogen bonding, O2, however, an opposite trend is observed. That is, the values of C_Q and δ_{iso} for O2 are much larger than those found in uracil crystals. In general, the calculated C_Q and δ_{iso} for the G- and U-quartets fit nicely in the correlation plot shown in Figure 5. However, we also found that the calculated ^{17}O quadrupole data for the G- and U-quartets deviate considerably from the correlation shown in Figure 6. More specifically, much smaller η_Q values are observed for the G- and U-quartets than those found for the nucleobase crystals. For example, for $C_Q = 8.087$ MHz (O4 in the G-quartet), the linear relationship in Figure 6 predicts a value of 0.600 for η_Q. Yet the actual value measured for O4 of the G-quartet is much smaller, $\eta_Q = 0.309$. This new relationship between C_Q and η_Q can probably be used as an indicator for the cyclic hydrogen-bond formation.

Comparison of ^{17}O Chemical Shifts in Different Phases. The ^{17}O chemical shift of a particular molecule often depends on the phase at which the NMR measurement is performed. A well-known example of this kind is the 36 ppm chemical shift difference between the ^{17}O NMR signals of water vapor and liquid water.[50] This large chemical shift change can be explained by the strong intermolecular hydrogen-bonding interaction between water molecules. For nucleobases, we have also observed large variations between the ^{17}O chemical shifts measured in liquid and solid states. It would be of interest to compare the ^{17}O chemical shifts in all three phases: gas, liquid, and solid. Unfortunately, experimental gas-phase NMR data for nucleobases are not available. However, it is probably a reasonable assumption that our theoretical data for isolated molecules with a fully optimized geometry can be used to mimic the gas-phase NMR data. In the discussion that follows, we refer to such calculated results (labeled as "opt" in Table 3) as the "gas-phase" data.

In Figure 9, we present the ^{17}O chemical shifts in different phases. Overall the ^{17}O chemical shifts exhibit a decrease from gas to liquid and to solid data. This is consistent with the expectation that the crystal lattice represents an environment where hydrogen bonding is the strongest. It is more informative

(47) See reviews: (a) Guschlbauer, W.; Chantot, J.-F.; Thiele, P. *J. Biomol. Struct. Dyn.* **1990**, *8*, 491. (b) Williamson, J. *Annu. Rev. Biophys. Biomol. Struct.* **1994**, *23*, 703.
(48) Cheong, C.; Moore, P. B. *Biochemistry* **1992**, *31*, 8406−8414.
(49) Meyer, M.; Steinke, T.; Brandl, M.; Sühnel, J. *J. Comput. Chem.* **2001**, *22*, 109.
(50) Raynes, W. T. *Mol. Phys.* **1983**, *49*, 443.

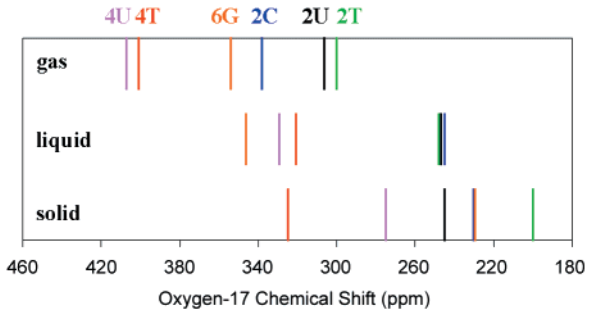

Figure 9. The relationship between the ^{17}O chemical shifts in gas, liquid, and solid states. The gas-phase data are the calculated results for single molecules fully optimized at the B3LYP/6-311G(d,p) level of theory. The liquid-phase data are experimental results in DMSO solutions. Chemical shifts are referenced to liquid H_2O.

to examine the chemical shift changes for individual compounds. The isotropic ^{17}O chemical shifts for O4 of thymine (labeled as 4T in Figure 9) have essentially the same values in the solid and solution states. However, the corresponding values for O2 of thymine (labeled as 2T) differ by approximately 50 ppm. This can be attributed to the fact that, in the solid state, O2 is directly involved in strong hydrogen bonding (Figure 3). As also seen in Figure 9, the gas-phase ^{17}O chemical shifts for O4 and O2 of thymine are shifted from their solution values by approximately the same amount, indicating that the degree of hydrogen bonding in solution is similar at O4 and O2. For uracil, chemical shifts for O2 and O4 also show very different variations. In particular, the gas-to-liquid chemical shift changes for O2 and O4 are comparable, 59 and 78 ppm. Yet the liquid-to-solid chemical shift changes for O2 and O4 are very different, 2 and 54 ppm. Cytosine also exhibits a large gas-to-liquid chemical shift change (93 ppm), but only a small liquid-to-solid change (37 ppm). This suggests that the hydrogen bonding of cytosine is quite strong in the liquid state. In contrast, O6 of guanine exhibits a negligible gas-to-liquid change (8 ppm), but a very large liquid-to-solid change (71 ppm), suggesting that the hydrogen bonding in guanine crystals is much stronger than that in solution. At the present time the interpretation of the above ^{17}O NMR data is only qualitative. However, as illustrated by Figure 9, the sensitivity of the ^{17}O NMR data to molecular structure and chemical bonding clearly has the potential to become an additional source of information about biomolecular structures.

4. Conclusion

We have presented a systematic solid-state ^{17}O NMR study for free nucleic acid bases. The present study demonstrates that it is feasible to obtain reliable solid-state ^{17}O NMR spectra for ^{17}O-enriched nucleobases and that ^{17}O NMR *tensors* are excellent indicators of hydrogen-bond formation. Even for seemingly similar functional groups, noticeable differences have been observed for ^{17}O NMR tensors. These spectroscopic features are potentially useful for probing base pairing in nucleic acids. The quantum chemical calculations have also helped identify the relationship between solid-state ^{17}O NMR tensors and molecular structure. The agreement between the experimental and calculated ^{17}O NMR tensors is reasonably good at the B3LYP/6-311++G(d,p) level of theory for models containing a complete hydrogen-bond network. Although the present study is concerned only with free nucleobases, extension to larger nucleic acid molecules is possible. It is anticipated that the availability of very high magnetic fields (18.8 T or higher) coupled with the advances in solid-state NMR methodology will significantly increase the feasibility of solid-state ^{17}O NMR in the study of biological macromolecules. It remains to be a challenge to chemists and biochemists to develop efficient synthetic techniques for introducing ^{17}O labels, site-specifically or uniformly, to molecules of biological importance.

Acknowledgment. G.W. thanks the Natural Sciences and Engineering Research Council (NSERC) of Canada for research and equipment grants. This research was partially supported by a grant to G.W. from the Advisory Research Committee of Queen's University. G.W. also thanks Queen's University for a Chancellor's Research Award (2000) and the Government of Ontario for a Premier's Research Excellence Award (2000). We are particularly grateful to Dr. Michael Meyer (Konrad-Zuse-Zentrum für Informationstechnik Berlin, Germany) for providing us with the atomic coordinates for optimized G- and U-quartet structures. We also thank Alan Wong for helpful discussion and assistance.

JA011625F